Biomimetic Tactile Sensor for Control of Grip

Nicholas Wettels, Djordje Popovic, Veronica J. Santos and Gerald E. Loeb
A.E. Mann Institute and Biomedical Engineering Department, University of Southern California
Los Angeles, CA 90089, USA, http://ami.usc.edu/

***Abstract* — We are developing a novel, robust tactile sensor array that mimics the human fingertip and its distributed set of touch receptors. The mechanical components are similar to a fingertip, with a rigid core surrounded by a weakly conductive fluid contained within an elastomeric skin. It uses the deformable properties of the finger pad as part of the transduction process. Multiple electrodes are mounted on the surface of the rigid core and connected to impedance measuring circuitry within the core. External forces deform the fluid path around the electrodes, resulting in a distributed pattern of impedance changes containing information about those forces and the objects that applied them. Here we report preliminary results with prototypes of the sensor, and we propose strategies for extracting features related to the mechanical inputs and using this information for reflexive grip control.**

***Index Terms*— Biomimetic, electrode impedance, pressure sensor, tactile sensor**

I. Introduction

The performance of prosthetic hands and robotic manipulators is severely limited by their having little or no tactile information compared to the human hand. A wide variety of technologies have been applied to solve the tactile sensing problem in robotics and medicine. Transduction mechanisms such as optics, capacitance, piezoresistance, ultrasound, conductive polymers, etc. have all yielded viable solutions but only for limited environments or applications. For example, most MEMS sensors provide good resolution and sensitivity, but lack the robustness for many applications outside the laboratory [1-3]. Beebe proposed piezoresitive silicon based MEMS sensor with a high tensile strength, but hysteresis and inability to sense shear force posed limitations [4]. Conductive particles suspended in elastomers can result in elastic materials whose resistivity changes with deformation. A recent enhancement of such materials called Quantum Tunneling Composites (QTC) greatly increases sensitivity and dynamic range but at the expense of mechanical hysteresis and simultaneous sensitivity to temperature and absorption of gases [5].

This research was funded by the Alfred E. Mann Institute for Biomedical Engineering at the University of Southern California and a grant from the National Academies Keck Futures Initiative. Please address correspondence to G.E. Loeb at 213-821-1112 or gloeb@usc.edu

The curved, deformable nature of biological finger tips provides mechanical features that are important for the manipulation of the wide variety of objects encountered naturally. Multi-axis force sensing arrays have been fabricated using MEMS but they are not suitable for mounting on such surfaces or for use in environments that include heavy loads, dust, fluids, sharp edges and wide temperature swings [2, 3]. If skin-like elastic coverings are placed on top of sensor arrays, they generally desensitize the sensors and function as low pass temporal and spatial filters with respect to incident stimuli [6]. Therefore, we considered it beneficial to make the cosmesis part of the transduction process rather than fighting it after the fact. This let us to the approach of using a fluid or gel filled pad in an elastomer as the transduction mechanism.

Helsel et al. have shown pressure sensation with an impedance based ionic fluid sensor using a grid of gold-chromium electrodes, ethylene glycol filler and latex skin while varying indentation along one dimension. This sensor was able to achieve resolution to 0.5 - 0.6 mm [7]. Russel also experimented with a variable impedance sensor, using electrodes on the elastomer “skin” interior and along the sensor core [8]. Fingertips that employ electrorheological fluids for dynamic shape control include plates to apply high voltage fields; these can also be used for capacitive sensing but practical arrays have encountered problems [9,10].

We describe a biomimetic tactile sensor that is sensitive to the wide range of normal and shear forces encountered in robotic and prosthetic applications. It is intrinsically simple, robust and easy to manufacture and repair.

II. Methods

A. Design Concept

Our tactile sensor is shaped like the fingertip and consists of a rigid central core surrounded by fluid and covered by a silicone elastomeric “skin” (Fig. 1). The skin is resistant to wear and possesses texture and tackiness similar to the properties that facilitate grip by biological fingertips. External forces deform the skin and weakly conductive fluid, causing changes in the electrical resistances measured by an array of electrode contacts distributed over the curved surfaces of the core. The impedance of each volume conductive path can be measured by applying an alternating current to each contact and measuring the resulting voltage drop with respect to a reference contact.

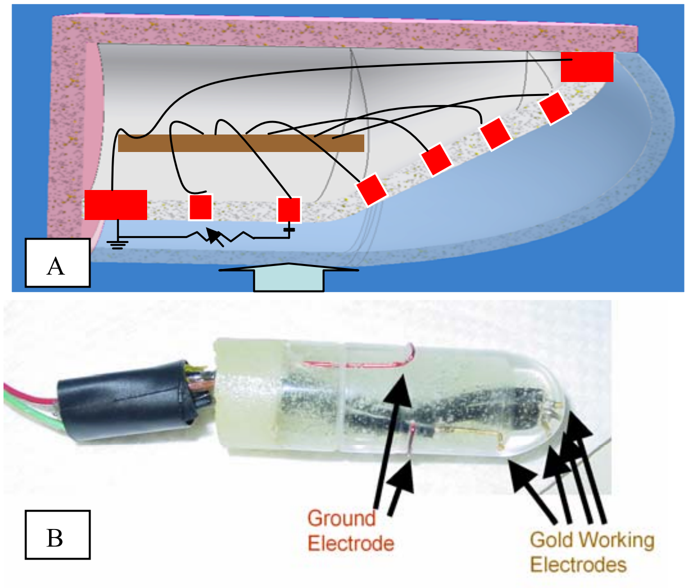

Figure 1: A) Mechanical drawing of the biomimetic tactile sensor showing a rigid core shaped like the distal phalanx (white) with an internal, sealed compartment for electronics (brown) connected to sensing electrodes (red) in contact with a weakly conductive fluid under a viscoelastic skin (light blue). B) Initial sensor prototype core with "skin" removed.

B. Prototype Fabrication and Theory of Transduction

The initial prototype contained four gold working electrodes and a wrap-around copper ground electrode. The gold electrodes were the cross-sectional area of wire with a diameter of .635 mm, whereas the copper electrode is a wire with a diameter of .406 mm. The wires were anchored in the walls of a machined acrylic body (13mm diameter, hemispherical end) that was subsequently filled with epoxy.

To build the next prototype (Fig 2), we machined a jeweler's wax mold whose shape is similar to the distal phalanx. Individual gold contacts were formed by melting the end of a 0.25mm gold wire with 5µ Parylene-C insulation into a ball and swaging to the desired diameter and contour. The contacts were tacked to the inside of the mold where desired and the wire lead was soldered to a multipin electrical connector. A capillary tube was affixed in the mold for later use to inflate the fingertip with fluid. The mold was filled with liquid dental acrylic and cured to form a rigid finger core with electrodes on its surface. Thus there are no moving parts and the sensing components and wiring are protected in a high- strength rigid core (compressive strengths 10-100 MPa and tensile strength 1 -10 MPa [11]).

Texturing of the internal surface of the skin (see below) can be created by abrading the surface of the rigid core if desired, followed by a mold-release coating. The fill-tube is loaded with fluid by capillary action and the fingertip is dip-coated in silicone to achieve the desired thickness of polymerized skin. A cap is screwed into the top of the core to act as the fingernail, anchoring the skin to the core on the dorsal side of the fingertip. The fill-tube is used to inflate the skin away from the core with the desired fluid. Mechanical fixation features can be incorporated into the mold to facilitate mounting of the fingertip to the mechatronic hand or to mechanical test instrumentation.

The sensitivity of the device depends complexly on the size of the electrode contacts, the conductivity of the fluid, and the viscoelastic properties of the combined system of skin and pressurized fluid. Lower viscosity provides higher sensitivity and frequency response. Lower conductivity provides higher sensitivity because the electrode impedance consists of two components in series: the metal-electrolyte interface, which is essentially a constant capacitance, and the volume-conductance of the surrounding fluid and space, which act as the variable resistance to be measured.

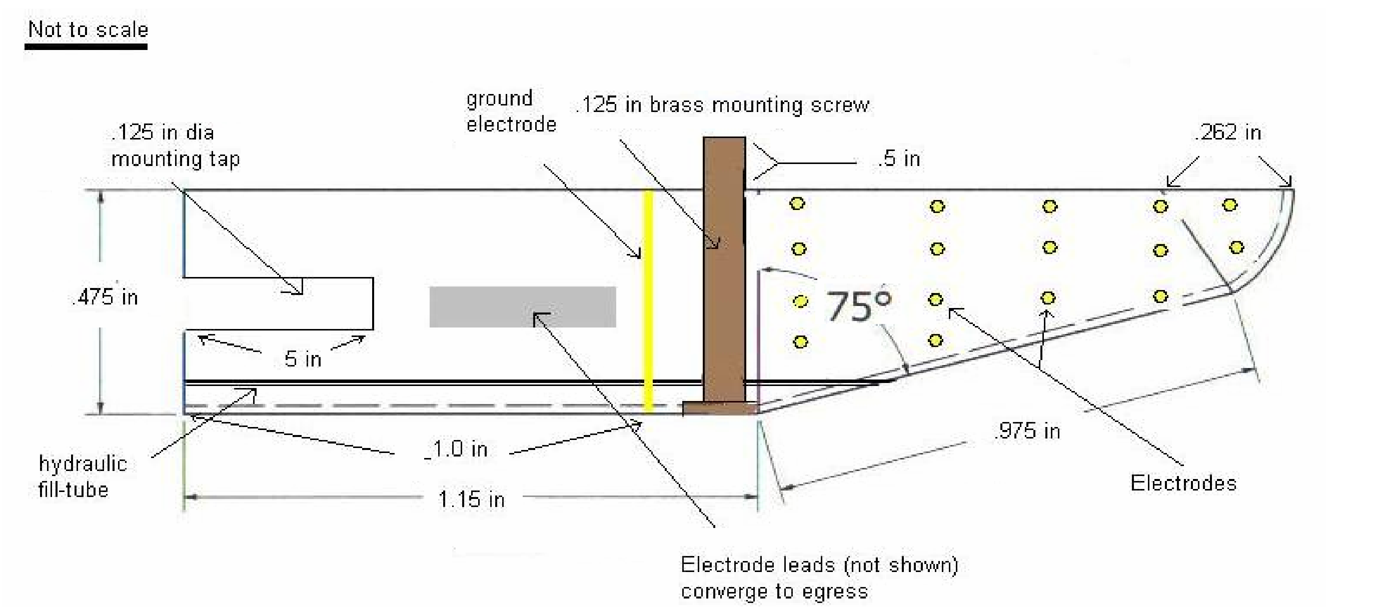

Figure 2. Mechanical Drawing of Second Prototype

Presently the fluid is a blend of glycol, water, sodium chloride and ethyl alcohol. Salt water acts as the conductor, glycol is a hygroscopic agent to preclude water loss by diffusion through the silicone elastomer and ethyl alcohol lowers the viscosity.

The choice of silicone elastomer for the skin depends on achieving mechanical properties and cosmetic appearance similar to normal skin. Candidate outer materials include Dragon Skin-Q by Smooth-On Inc. (Shore A hardness = 10 and tear strength = 102 lbs per inch) and VST-30 by Factor II Inc. (Shore A hardness = 23 and tear strength = 100 lbs per inch). A higher durometer inner coating can be used to optimize mechanical properties, while the softer, outer coatings will provide a more cosmetic appearance and feel.

Adjusting the thickness and viscoelasticity of the covering skin and contouring its inside surface has complex effects on the dynamic range and two-point discrimination of the array (see below). Attaching the skin to the dorsum in the manner of a fingernail and positioning sensor electrodes on the curved surface of the core adjacent to this restriction causes these lateral-facing electrodes to respond selectively to tangential forces applied at the fingertip. Such forces cause sliding of the skin over the core, constricting the fluid on one side of this "nail bed" and bulging it on the other, similar to a biological fingertip. The number and distribution of electrodes required to sample these phenomena efficiently remain to be determined.

The strategy of dip-coating elastomeric skin onto the rigid core offers the advantage of easy repair of the most vulnerable part of any finger. It should be possible to replace the skin without affecting the sensing electrodes or their supporting electronic circuitry within the rigid core.

C. Signal Conditioning

The electrical impedance between a single working electrode contact and a large reference electrode can be modeled by the circuit below (Fig 3).

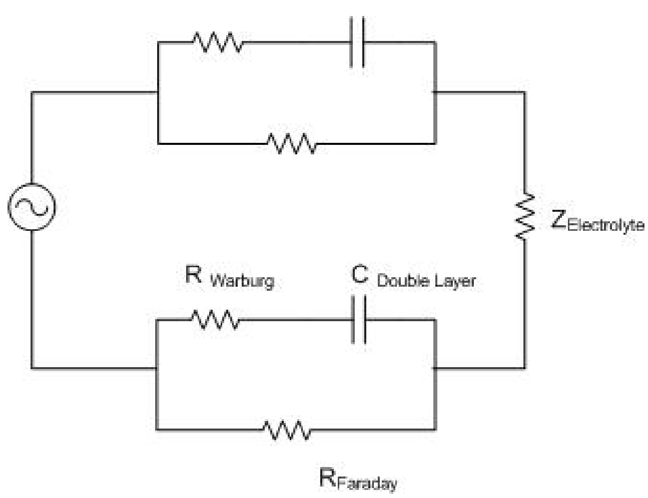

Figure 3: Generic model of a working electrode, electrolyte and counter-electrode.

It is desirable to energize the electrode system in such a way that the voltages developed across the double-layer capacitances are sufficiently low so as to avoid Faradaic current flow [12]. Faradaic current through metal-electrolyte junctions tends to produce corrosion of the metal contacts and electrolysis of the electrolyte. By applying low alternating currents at reasonably high frequencies, the peak voltage across the double-layer capacitors can be kept low and the Faradaic resistors can be ignored. This leaves the double layer capacitance of both electrodes and the resistance of the electrolyte in series. The capacitance per unit area of our electrodes lies between 10 and 100 $\mu F/cm^2$ [13, 14]. For a single electrode contact 1 mm in diameter; the impedance at 5 kHz will be on the order of 100 Ω. This is negligible compared to the dynamic range of the sensor's resistivity (10 – 800 kΩ in the prototypes described below). The impedance for the counter-electrode will be even smaller because it is larger and possesses an even greater capacitance.

The detection circuit (Fig. 4) is driven with a 5kHz 10VAC sine wave in series with R1, which acts as a current source over the lower impedance range of the sensor. Based on the dynamic range of sensor impedances measured, a 1MΩ resistor was chosen for R1. The envelope magnitude of the sinusoidal signal is demodulated by the active rectifier (op amp LMC 6482) to provide Vout. C1 is a blocking capacitor that removes any DC bias from the sensor electrodes to prevent corrosion and electrolysis. The time constant of the filter R2C2 was chosen to be 0.1 ms. This is based on physiological experiments that showed that the loading phase of a grip was never shorter than about 200ms [15]. The resistor R3 serves to discharge the capacitor C2 when the diode is not conducting. In an array of such electrodes, most of the circuitry can be electronically multiplexed among rather than duplicated for each electrode.

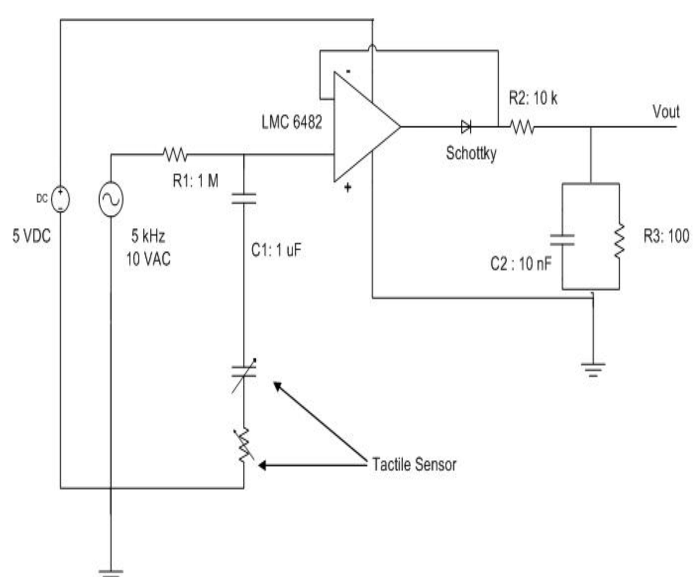

Figure 4: A circuit diagram of a single sensor channel.

D. Probe Experiments

To determine static characterization of a single electrode, normal forces were applied to the array at a calibrated distance from the electrode of interest. A three-axis manipulator was used to advance interchangeable probes: 2mm diameter with 1mm radius of curvature, 20mm diameter with 11.5 mm radius of curvature, and a large flat plate (9.67 cm^2). The probes were chosen to have radii of curvature much small than, approximately equal to and much larger than the curvature of the tactile array, respectively. Deflection was recorded from point of first contact with the skin. Vertical force was measured by an AMTI HE6X6 six-axis forceplate under the clamp for the fingertip (Fig. 7).

.

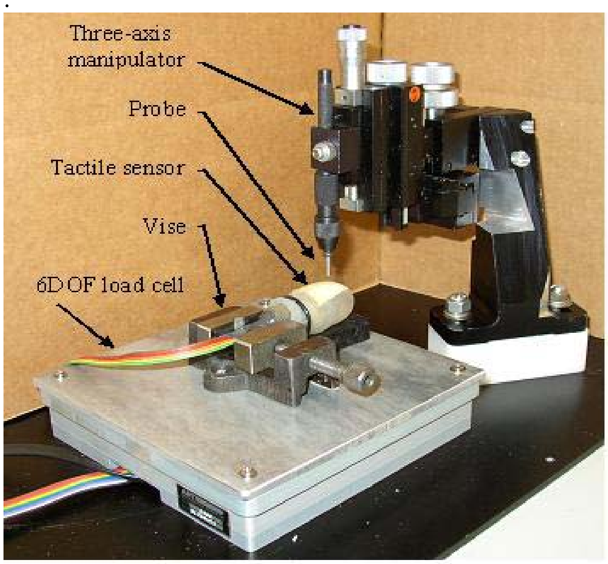

Figure 7: Test set-up with force meter, manipulator and tactile sensor.

The data are reported here as the actual electrode impedance for the design illustrated in Figure 1B, except Fig. 12, which represents the output of the signal conditioning circuitry illustrated in Figure 4. The skin of this sensor was a triple dip-coat of VST-30 silicone elastomer with internal texturing consisting of a thin layer of commercial latex with an array of 0.8mm high pyramidal bumps spaced approximately 2mm apart. The sensor was inflated with 3.5mL of a dilute NaCl solution (0.75g/l; 1/12th the concentration of physiological saline).

III. Results

A. Single Electrode Static Characterization

1) Deflection Applied Directly Above Electrode

As the fingertip is compressed, there is a monotonic but nonlinear increase in electrode impedance over a range of 10-100 times the starting value (Figure 8). The slopes depend complexly on the curvature of the probe, as discussed below. The reaction force of the fingertip also rises monotonically and nonlinearly as the fluid is displaced from under the skin (regions labeled A in Figures 8 & 9) and then the skin is compressed against the rigid core (regions B and C). This results in the impedance vs. force curves illustrated in Figure 9 for the same trials as Figure 8. Interestingly, the sigmoidal shape of these logarithmic curves is reminiscent of many biological transducers, which generally need to optimize local sensitivity over a wide dynamic range of possible inputs.

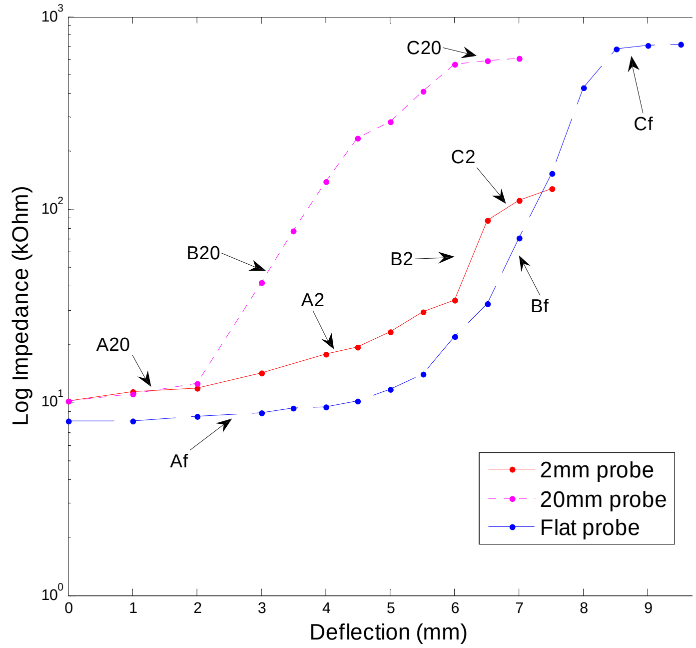

Figure 8: Log impedance (1-1000 kΩ) versus static deflection of skin applied by three probes with different curvatures. Three distinct operating regions (labeled A, B and C) are present for each curve and discussed in text.

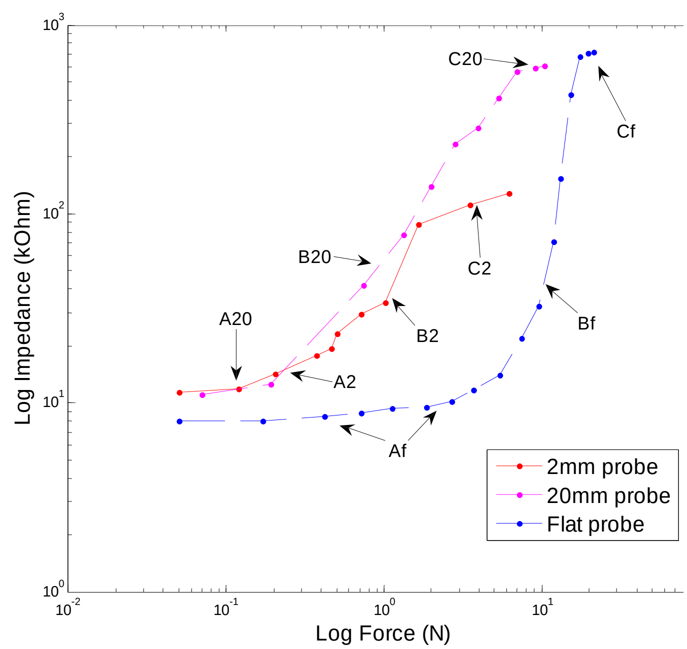

Figure 9: Log Impedance versus log force (0.01-100N) normal to skin surface for same deflections as in Figure 8.

2) Deflection Applied Above and Around Electrode

The sensor was systematically probed in a 3 by 4 grid at 2 mm increments to a skin deflection of 5.5 mm using the 2mm probe. This was done about an electrode located at X = 7.5 and Y = 15 mm to show sensitivity to nearby deformations (Figure 10).

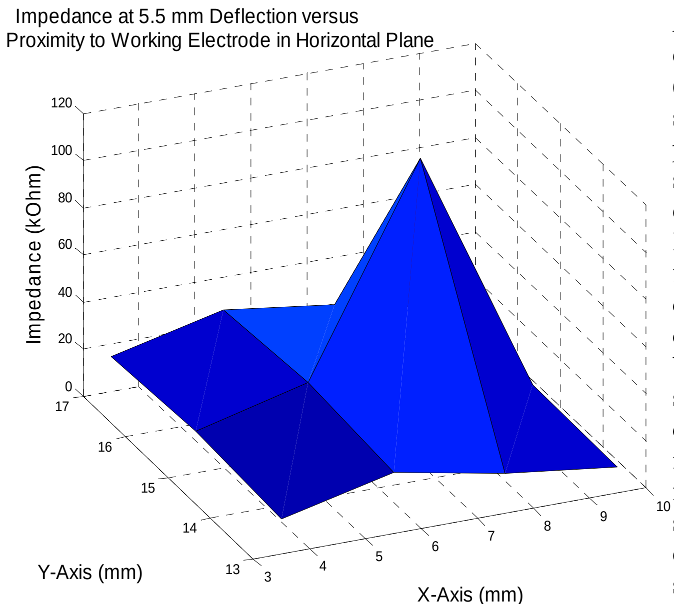

Figure 10: Impedance as a function of center of pressure with respect to the electrode location.

3) Two- Electrode Response to Rolling Motion

As a crude test of the distribution of responses across multiple electrodes, the prototype sensor was rolled over an Inastomer force sensitive resistor while observing the rectified and filtered signals from multiple electrodes on an oscilloscope.

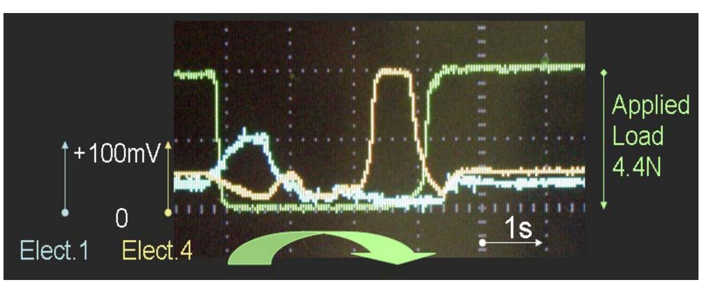

Figure 11: Two-electrode Sensor Output During Roll

As the skin deformation rolls over Electrode 1, its impedance increases. The pressurized skin bulges over Electrode 4, so its impedance decreases. Later as the roll reaches Electrode 4, the reverse occurs.

IV. DISCUSSION

As illustrated in Fig. 8 and 9, the response of the sensor varies significantly with radius of curvature and contact surface area of the incipient object, but generally consists of three phases. During the initial deflection of the skin, the fluid is displaced from between the skin and the core but the shape of the remaining conductive path depends on the shape of the probe. For the 20mm probe (similar in curvature to the core), there is a gradual rise of impedance and force (region A20) for the first 2mm of deflection until the skin contacts the electrode. Then the impedance and the force rise rapidly (region B20) as the textured inner-surface of the skin starts to seal to the electrode (plateau at region C20). For the 2mm probe, the gradually rising portion is longer (A2) because the small probe deforms the inner contour of the skin, preventing even contact over the entire electrode surface until it reaches a larger deflection (B2). Even then there is a residual film of fluid preventing saturation (C2) as the skin is further deformed by the small probe. In the case of the flat probe, we do not see the rapid increase in impedance until ~4.5 mm because the flat surface is causing global deformation of the sensor body (Af). Not only is the probe pushing the fluid downward, but it is also pushing it outward, causing a change in the shape, but little change in impedance of the volumetric flow-path. Eventually the skin contacts the core, producing a steeper increase in both impedance and force (Bf) and eventual saturation (Cf). The force at which the sensor saturates depends on the texture and hardness of the inner surface of the skin and the force per unit contact area that deforms this texture.

It would appear that there is an ambiguity between impedance and deflection (or force) and the shape of the contacting object. If the shape of the object is not known *a priori*, how is one to determine deflection or force from impedance? This problem is solved by actively exploring the object with the sensor to obtain other features such as object shape – which is exactly what the human haptic system does. The amount and timing of the deflection is caused by and known to the operator exploring the object. Thus the shape can be extracted from the time course of the impedance measured; probably by comparing the responses with the expectation based on *a priori* knowledge and hypothesis (see also Object Hardness/Softness below).

We also observe impedance changes when deformations occur around the electrode, demonstrating the ability to sense deformations outside the electrode's immediate vicinity. This is consistent with the hypothesis regarding the flat probe behavior previously described. Fig. 10 shows that the highest impedance value was measured when the probe deflected the skin directly above the electrode of interest.

The ability to resolve information about place and motion of center of displacement is possible when observing deformations about two electrodes simultaneously. As shown in Fig.11, the rolling motion caused global deformations that were observable at both electrodes. This is not unlike the behavior of the human finger pad when a human uses a precision grip to lift a small object. One part of the finger pad is squeezed towards the distal phalanx and the other bulges. Our sensor is able to represent such phenomena and encode features like these into a spatial pattern of electrical signals related to two-point discrimination as described in human subjects. This suggests (but does not yet demonstrate) that the tactile array will be capable of two-point discrimination with a resolution comparable to the thickness of the skin itself.

A. *Feature Extraction*

The positioning of the electrodes with respect to the contours of the core and overlying fluid and skin causes distinct patterns of change in the various impedances measured by the detection circuitry as the sensor assembly contacts various objects and surfaces with various force vectors. For example, those electrodes located on the most convex portions of the core near the seals of the skin will detect large increases in impedance when shear forces are directed away from them, pulling the skin close to these electrodes. The following section summarizes phenomena of the device that, in principle, can be used to extract information about an object.

Contact force: As the total force increases on the central area of the sensor assembly, the fluid will be squeezed. The fluid overlying the electrodes in the compressed central area of the sensor assembly becomes thinner, causing the impedance measurements associated with those electrodes to become higher. The sum of all such impedance increases is related to the total force of contact; that sum will be dominated by the nonlinear increase in impedance as electrodes approach the skin.

Location of force centroid: The impedance increases associated with the contact force measurement above can be related to the position of the electrodes in the array in order to estimate where the center of force is located on the surface of the sensor assembly.

Shape of external object: If the contacting object is not radially symmetrical, the distribution of impedance changes detected by the electrodes will be similarly asymmetrical. The spatial pattern will also be related to the radius of curvature of the contacting object. For example, a small or narrow object will produce a local deformation of the skin that will cause large changes of impedance for only one or a few electrodes close to the point of contact. A sharp edge will cause an abrupt boundary between electrodes with high impedance and those with low impedance (as a result of displacement of fluid and bulging of the skin).

Vector of force: In most object-manipulation tasks, the force between the sensor assembly and the contacted object is not oriented normal to the surface of the sensor assembly. In biological skin, shear force components change the stress and strain distributions within the fingertip that are sensed by receptors located within dermal and subdermal tissues but also by the distribution of pressure around the perimeter of the finger pad, particularly where the skin is anchored by the nail bed [16].

In our tactile sensing finger tip, those electrodes located on the most convex portions of the core near the seals of the skin will detect large increases in impedance when shear forces are directed away from them. Such force will cause the skin to slide, compressing the fluid over these electrodes. A deviation of the force vector from normal is generally associated with a tendency of the grasped object to slip or rotate [17, 18].

Vernier detection of force shifts: The detection of imminent slip is essential to the maintenance of efficient and effective grip on objects, in which it is generally desirable to produce only the minimal force on the object required to initiate and maintain stable grasp. In the biological fingertip, imminent slip is detected by localized, tiny shifts in the distribution of shear forces in the skin. The relationship between electrode impedance and thickness of the overlying fluid is inherently highly nonlinear, as described above. For example, if the inner surface of the nonconductive, elastomeric skin actually touches and covers an electrode, its impedance with respect to any other contact increases abruptly towards infinity.

By incorporating protruding textural elements such as bumps and ridges onto the inner surface of an elastomeric skin, the distribution of impedances across the array of electrodes will undergo large changes when the skin is compressed against the core. If the spatial pattern of this texture is regular but slightly different from the spatial pattern of the electrodes, small lateral shifts will cause large changes in the spatial pattern of impedances across the electrode array, similar to the small shifts that can be detected by a Vernier pair of scales. It is important to note that the critical event to be detected is the *onset of any change* in the shear force distribution, not the actual shear forces or the direction of the change [19].

Contact Transients and Vibration: Biological skin contains specialized Pacinian receptors that are highly sensitive to the acceleration component of skin deformation, making them useful to detect transient mechanical events that occur when making and breaking contact between a held object such as a tool and another object, and vibration of skin induced by the motion of skin ridges sliding over a textured object surface, which can be used to yield a sense of roughness of the surface being explored. The impedance of the electrodes in the biomimetic fingertip will undergo only very small changes when lightly loaded, but it may be possible to detect such changes by means of their synchronous phasing across the entire array of electrodes [20]. Various signal-averaging techniques can be applied to enhance the detection of the correlated component of weak and noisy signals from an array of sensors (but see below for hydrostatic pressure measurement).

Object Hardness/ Softness: As noted in Fig 8, the sensor responds dramatically to light deformation. As previously stated, the sensor can detect mechanical transients associated with making contact with an object. If the sensor is affixed to a mechatronic finger moving at a known velocity, the rate of deformation increase can be used to indicate the level of hardness or softness of a contacted object. A hard object will cause a rapid increase in deformation (and voltage response) for a given finger velocity when compared to a soft object.

B. Further feature characterization

We have shown basic characterization of the sensor with respect to force, deflection and impedance. More thorough testing is required (including thermal response, destructive analysis, etc.). We have yet to undertake systematic dynamic testing, but hysteresis and drift are not expected in our sensor because the silicone elastomer is a spring-like material that does not exhibit creep and the fluid has low viscosity.

Some information (particularly about position such as force centroids and areas) could be extracted analytically, based on a reasonable mathematical model. Our sensor array has properties similar to the biological fingertip, however, so it will likely require non-analytical signal processing methods similar to those employed by the biological nervous system. The temporospatial distribution of activity in the biological touch sensors depends complexly on the inherent sensitivity of the sensors, their distributions throughout the tissues of the fingertip and the forces that the fingers apply to external object, as well as on the nature of the external object itself. Similarly, in our array of tactile sensors, force magnitude and location interact with each other. For example, the same force vector applied close to the nail bed will create a different amount of net impedance change than if applied to the fingertip; the total change in impedance cannot be used as a measure of the applied force unless corrected for the position. At higher force levels the information about position may be blurred because of nonlinear changes in electrode impedance as the inside surface of the skin makes contact with the electrodes. This is similar to the saturation of light touch receptors and the need to incorporate information from deep touch and nociceptors in biological skin.

The characterization experiments described above will produce a rich data set consisting of pairs of input vectors (describing location and components of applied force) and output vectors (voltages related to impedances of the electrode array). These will be used to train neural networks for various tasks. This approach can be use to determine the discriminability of various input conditions or, conversely, to determine the ability to generalize a single parameter such as magnitude of forces applied to different portions of the finger tip. For the force intensity extraction, a multi-layer perceptron (MLP) and radial-basis neural network will be used initially because both have proven to be able to approximate any given non-linear relation when a sufficient number of neurons are provided in the hidden layer [21, 22]. For the mapping of force localization on the finger surface, a Kohonen network would also be feasible [23]. Two-point discrimination is also likely to be possible but will depend critically on the thickness and viscoelastic properties of the skin.

C) Enhancements

In addition to the primary array of electrodes and electrolyte, this system is capable of being easily fitted with enhancements and auxiliary systems to provide further sensory information.

To enhance vibration sensing, dermal ridges (i.e. fingerprints) can be molded onto the exterior of the elastomer. Human ridges are typically .1 mm in height and .3 - .5 mm in width and aid in sensing of rough surfaces [24]. Mukaibo *et al.* showed successful application of this principle in their tactile sensor that included a solid distal phalanx coated in a silicone elastomer [25]. They convert texture into vibration during the stick-slip phenomena as the ridges are run over an object's surface, which is detected by the Meissner corpuscles below the epidermal ridges. The frequency of the vibration is:

$$f = v / \lambda \qquad (1)$$

where f is frequency; v is finger velocity and λ is peak-to-peak distance between ridges. Such small amplitude vibrations will produce coherent signals in the various contact impedances but their amplitudes will be small and may be difficult to detect. Alternatively the pressure in the fluid as a whole could be sensed by incorporating a hydraulic pressure sensor on the end of the fill-tube, doubly acting as its plug. A commercial sensor such as Silicon Microstructures' SM 5822 is ideal for this purpose.

Thermal sensing is also desirable as a part of haptics and could be incorporated in several ways. Saline solutions tend to increase their volume conductivity at higher temperatures (the reverse of solid-state resistors) so it may be necessary to incorporate a thermistor on the surface of the core to adjust the calibration of the impedance sensing. Alternatively, the resting distribution of electrode impedances will reflect ambient temperature. Conventional thermistors mounted on the core will tend to respond slowly to contact with hot or cold objects because the heat capacity of the surrounding fluid and skin will reduce their sensitivity to external objects. It may be necessary to mount a thermistor on the skin itself, a problem that must be solved for any gripping surface that includes a viscoelastic pad to help stabilize contact with objects. For haptic characterization of the material properties of objects, humans actually use heat flow from body temperature, so a heated thermistor may be necessary.

V. USE OF THE TACTILE INFORMATION

Stabilizing grip is an important function whose requirements and natural strategies are starting to be well understood. In a series of papers by Roland Johansson and coworkers, it has been shown that the grip stability is affected by an object's size and shape, its mass and weight distribution, and by the coefficient of friction between the fingertips and surface of the object [26-28]. They have also shown that the central nervous system usually adjusts the grip force so that the friction force developed between the fingertips and the object surface has only a small margin over the external forces that would otherwise cause the object to slip [15, 29]. This strategy is energetically efficient and suitable for manipulating delicate objects that might be crushed, but it demands continuous tactile sensing and adjustment of grip forces according to the perceived properties of the gripped object.

Each finger's grip force is adjusted independently based on the sensory information from that finger only and on the local conditions in terms of weight distribution and friction. At least some of this adjustment occurs so rapidly that it appears to be mediated reflexively in the spinal cord rather than via the brain. This is important for prosthetic limbs because it suggests that tactile information can serve a useful function even if communication channels to provide conscious perception of touch to the operator remain nonexistent or primitive, as they are now. Algorithms for the automatic adjustment of grip using biomimetic strategies are likely to be valuable also in telerobotic and purely robotic manipulanda.

Figure 12: Sarcos Robotic Arm performing the sort of object manipulation task for which rapid, closed-loop adjustment of grip forces is likely to prove useful.

We plan to integrate our tactile sensors into the three fingertips of a Sarcos robot (illustrated in Fig. 12) and train neural-network based controllers to produce patterns of grip force adjustment that mimic those described in psychophysical experiments on human subjects. Fortunately, there is now a rich database describing grip forces and their adjustment behaviors in human subjects coping with both predictable and unpredictable pulling loads [15, 28 - 30]. One strategy for the controller divides the problem into two levels, one trained to extract information about force intensity and distribution (as described in Section IV.A.1.), and a higher level block trained to adjust grip forces based on the extracted sensory information. Another strategy would be to train the robotic hand to behave like a human hand using the raw data from the sensor array as the input layer to the neural network.

Realistic grip control will require higher-level strategies than reflexive adjustment. There are perhaps better embodied by discontinuous state machines than by continuous neural networks. Humans can modulate their grip adjustment reflexes to provide a variable margin of safety or to allow voluntary release of objects. Humans confronted with a novel object adopt exploratory strategies, slowly decreasing grip force until subtle changes in the distribution of forces in the skin signal incipient slip. Humans adopt iterative haptic exploration strategies in which sensory information returned from one exploratory movement of the hand is used to devise the next exploratory movement. Humans learn to use all available tactile information during an extended period of development and skill acquisition. Substantive changes in this tactile information (e.g. as a consequence of injuries to the fingers or their peripheral nerves) require lengthy therapeutic retraining to achieve functional rehabilitation.

CONCLUSION

The biomimetic fingertip described in this report will not by itself solve any of the above problems of object manipulation and identification. It does provide a mechanically robust and informatically rich set of sensors that bears some resemblance to the biological tactile sensors. Most of the tools and tasks of an industrial world were designed by humans to be performed by human hands. This motivates the strategy of biomimetic design for robotic and prosthetic hands intended to function in this world.

ACKNOWLEDGEMENTS

The authors are grateful to the Alfred E. Mann Institute for Biomedical Engineering at the University of Southern California for assistance with this project.

REFERENCES

[1] Lee M.H., Nichols H.R., Tactile sensing for mechatronics – a state of the art survey. *Mechatronics* 9:1-31 1999.

[2] Beccai L., Design and fabrication of a hybrid silicon three-axial force sensor for biomechanical applications *Sensors and Actuators A: Physical. Vol. A120, no. 2*: 370-382. 17 May 2005

[3] Mei T. Et al. An integrated MEMS three-dimensional tactile sensor with large force range. *Sensor and Actuators 80:*155-162, 2000.

[4] Beebe D., Hsieh, Denton D., Radwin R. A silicon force sensor for robotics and medicine. Sensors and Actuators A 50:55-65, 1995.

[5] Bloor D., Donnely K., Hands P.J., Laughlin P., Lussey D. A metal-polymer composite with unusual properties. *Journal of Physics D: Applied Physics*, 38: 2851-2860, 2005.

[6] Vasarhelyi G., Adam M., Vazsonyi E., Barsony I., Ducso C. Effects of the elastic cover on tactile sensor arrays. *Sensors and Actuators132:*245-251, 2006.

[7] Helsel, M; Zemel, J N; Dominko, V An impedance tomographic tactile sensor. *Sensor and Actuators*. Vol. 14, No. 1, pp. 93-98. 1988

[8] Russell, R.A. Parkinson, S. Sensing surface shape by touch. *IEEE International Conference on Robotics and Automation*. Vol.1 423-428, 1993.

[9] Kenaly G., Cutkosky M. Electrorheological fluid-based robotic fingers with tactile sensing. *Proceedings of IEEE International Conference on Robotics and Automation* 1:132-136, 1989.

[10] Voyles R., Fedder G., Khosla P. Design of a modular tactile sensor and actuator based on an electrorheological gel. *Proceedings of IEEE International Conference on Robotics and Automation 1*:132-136, 1989

[11] Lee Y.K., Lim, B.S., Kim, C.W. Mechanical properties of calcium phosphate based dental filling and regeneration materials *Journal of Oral Rehabilitation* 30; 418–425, 2003.

[12] D. Merrill, M. Bikson, J. Jeffreys, Electrical stimulation of excitable tissue: design of efficacious and safe protocols. *Journal of Neuroscience Methods,* 141: 171-198, 2005

[13] A. Dalmia, C.C. Liu, R.F.Savinell Electrochemical behavior of gold electrodes modified with self-assembled monolayers with an acidic end group for selective detection of dopamine. *Journal of Electrochemistry,* 430: 205-214, 1997

[14] B. Piela, P. Wrona, Capacitance of the gold electrode in 0.5 M sulfuric acid solution: AC impedance studies. *Journal of Electrochemistry,* 388: 69-79, 1994

[15] Johansson R., Riso R., Hager C. and Backstrom L. Somatosensory control of precision grip during unpredictable pulling loads. I Changes in load force amplitude, *Experimental Brain Research* 89: 181-191, 1992

[16] Birznieks I., Jenmalm P., Goodwin A.W., Johansson R.S. Encoding of direction of fingertip forces by human tactile afferents. *Journal of Neuroscience*. 21:8222-8237, 2001.

[17] Flanagan J.R., Burstedt M.K.O., Johansson R.S. Control of fingertip forces in multi-digit manipulation. *Journal of Neurophysiology*. 81:1706-1717, 1999.

[18] Johansson R.S., Westling G. Roles of glabrous skin receptors and sensorimotor memory in automatic control of precision grip when lifting rougher or more slippery objects. *Experimental Brain Research*. 56:550-564, 1984.

[19] Johansson R.S., Westling G. Signals in tactile afferents from the fingers eliciting adaptive motor responses during precision grip. *Experimental Brain Research*. 66:141-154, 1987.

[20] Westling G., Johansson R.S. Responses in glabrous skin mechanoreceptors during precision grip in humans. *Experimental Brain Research*. 66:128-140, 1987.

[21] K. Hornik, M. Stinchcombe, and H. White. Multilayer feed forward networks are universal approximators.
Neural Networks, 2(5):359-366, 1989.

[22] Park, J. and I. Sandberg, Approximation and radial-basis-function networks, *Neural Computation* 5, 305-316, 1993.

[23] Caudill, M.; Butler, C. Understanding Neural Networks: Computer Explorations; Volume 1: *Basic Networks*; The MIT Press; Cambridge, Massachusetts, 1992.

[24] D. Yamada, T. Maeno and Y. Yamada, Artificial Finger Skin having ridges and distributed tactile sensors used for grasp force control, *Proc. IEEE/RSJ International Conference on Intelligent Robots and Systems*, pp. 686-691, 2001.

[25] Y. Mukaibo, H. Shirado, M. Konyo, T. Maeno Development of a texture sensor emulating the tissue structure and perceptual mechanism of human fingers. *Proc. of the 2005 IEEE International Conference on Robotics and Automation*, pp. 2576-2581, 2005.

[26] Johansson R.S. and Westling G. Role of glabrous skin receptors and sensorimotor memory in automatic control of precision grip when lifting rougher and more slippery objects, *Experimental Brain Research* 56: 550-564, 1984

[27] Cole K.J., Johansson R. Friction at the digit-object interface scales the sensory-motor transformation for grip responses to pulling loads, *Experimental Brain Research*, 95: 523-532, 1993.

[28] Johansson R., Hager C. and Riso R. Somatosensory control of precision grip during unpredictable pulling loads. II Changes in load force rate, *Experimental Brain Research* 89: 192-203, 1992.

[29] Gordon A., Westling G., Cole K.J. and Johansson R. Memory representation underlying motor commands used during manipulation of common and novel objects, *Journal of Neurophysiology* 69: 1789-1796, 1993.

[30] Johansson R.S., Birznieks I. First spikes in ensembles of human tactile afferents code complex spatial fingertip events. *Nature Neuroscience* 7:170-177, 2004.

[31] Butterfass, J., Grebenstein M., Lui H., Hirzinger G. DLR-Hand II: Next generation of a dexterous robot hand. *Proceedings of the IEEE International Conference on Robotics and Automation.* pp 109-114, 2001